

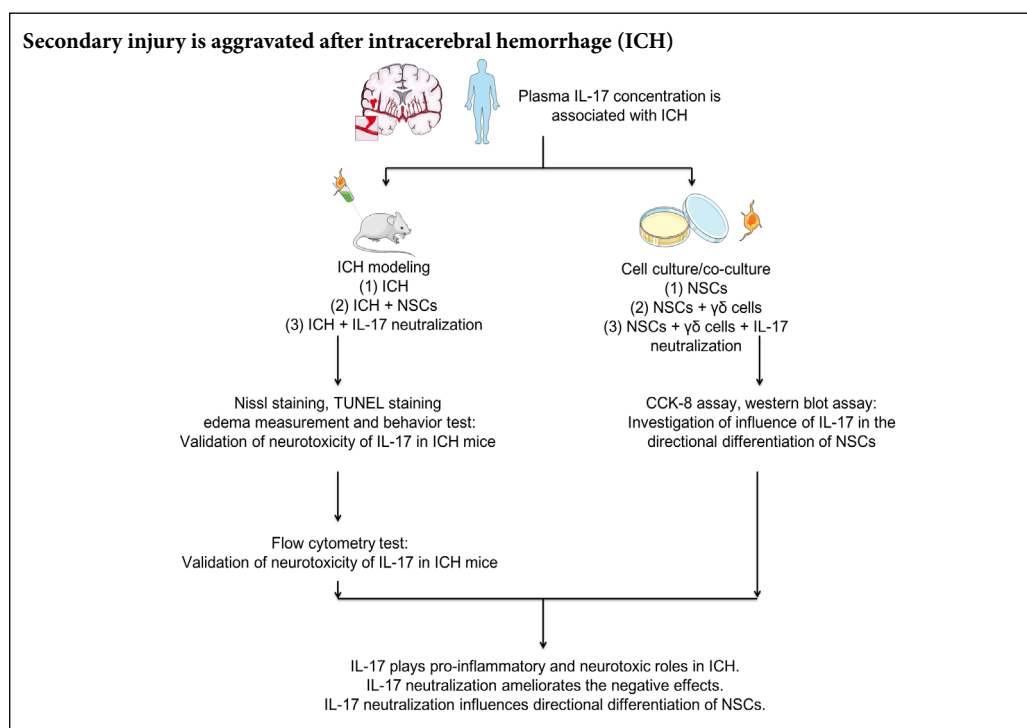
# Neurotoxic role of interleukin-17 in neural stem cell differentiation after intracerebral hemorrhage

Lu Gao<sup>‡</sup>, Ping-Ping Li<sup>‡</sup>, Tian-Yu Shao, Xiang Mao, Hao Qi, Bing-Shan Wu, Ming Shan, Lei Ye<sup>\*</sup>, Hong-Wei Cheng<sup>\*</sup>

Department of Neurosurgery, First Affiliated Hospital of Anhui Medical University, Hefei, Anhui Province, China

**Funding:** This study was supported by the Natural Science Foundation of Anhui Province of China, No. 1708085MH211 (to HWC); the College Top-notch Talent Foundation of Anhui Province of China, No. KJ2018A0207 (to HWC).

## Graphical Abstract



**\*Correspondence to:**

Hong-Wei Cheng, MD,

hongwei.cheng@ahmu.edu.cn;

Lei Ye, MD, yelei8778@sina.cn.

#Both authors contributed equally to the study.

**orcid:**

0000-0001-8239-3941

(Hong-Wei Cheng)

0000-0002-5079-8730

(Lei Ye)

**doi:** 10.4103/1673-5374.272614

**Received:** July 24, 2019

**Peer review started:** July 26, 2019

**Accepted:** October 26, 2019

**Published online:** January 9, 2020

## Abstract

Interleukin 17 (IL-17) and its main producer, T cell receptor  $\gamma\delta$  cells, have neurotoxic effects in the pathogenesis of intracerebral hemorrhage (ICH), aggravating brain injuries. To investigate the correlation between IL-17 and ICH, we dynamically screened serum IL-17 concentrations using enzyme-linked immunosorbent assay and explored the clinical values of IL-17 in ICH patients. There was a significant negative correlation between serum IL-17 level and neurological recovery status in ICH patients ( $r = -0.498$ ,  $P < 0.01$ ). To study the neurotoxic role of IL-17, C57BL/6 mice were used to establish an ICH model by injecting autologous blood into the caudate nucleus. Subsequently, the mice were treated with mouse neural stem cells (NSCs) and/or IL-17 neutralizing antibody for 72 hours. Flow cytometry, brain water content detection, Nissl staining, and terminal deoxynucleotidyl transferase-mediated dUTP nick end labeling results indicated that NSC transplantation significantly reduced IL-17 expression in peri-hematoma tissue, but there was no difference in T cell receptor  $\gamma\delta$  cells. Compared with the ICH group, there were fewer apoptotic bodies and more Nissl bodies in the ICH + NSC group and the ICH + NSC + IL-17 group. To investigate the potential effect of IL-17 on directional differentiation of NSCs, we cultured mouse NSCs (NE-4C) alone or co-cultured them with T cell receptor  $\gamma\delta$  cells, which were isolated from mouse peripheral blood mononuclear cells, for 7 days. The results of western blot assays revealed that IL-17 secreted by T cell receptor  $\gamma\delta$  cells reduced the differentiation of NSCs into astrocytes and neurons, while IL-17 neutralization relieved the inhibition of directional differentiation into astrocytes rather than neurons. In conclusion, serum IL-17 levels were elevated in the early stage of ICH and were negatively correlated with outcome in ICH patients. Animal experiments and cytological investigations therefore demonstrated that IL-17 probably has neurotoxic roles in ICH because of its inhibitory effects on the directional differentiation of NSCs. The application of IL-17 neutralizing antibody may promote the directional differentiation of NSCs into astrocytes. This study was approved by the Clinical Research Ethics Committee of Anhui Medical University of China (For human study: Approval No. 20170135) in December 2016. All animal handling and experimentation were reviewed and approved by the Institutional Animal Care and Use Committee of Anhui Medical University (approval No. 20180248) in December 2017.

**Key Words:** antibody neutralization; astrocytes; directional differentiation; interleukin 17; intracerebral hemorrhage; neural stem cells; Nissl staining; recovery; T cell receptor  $\gamma\delta$  cells; TUNEL staining

**Chinese Library Classification No.** R453; R364; R363

## Introduction

Spontaneous intracerebral hemorrhage (ICH) is a generic term for a range of devastating brain hemorrhagic diseases that can be caused by non-traumatic events, such as hypertension, vascular malformation, or for unknown reasons (Neves et al., 2018). The incidence of spontaneous ICH is 8–15% of all strokes in high-income countries, but has a higher percentage in Asia. Spontaneous ICH often has a poor outcome, with a one-month mortality rate of 30–55% and the highest burden of disability-adjusted life years among all stroke types (Krishnamurthi et al., 2014; Chen et al., 2017). Although therapeutic technologies have been developed in recent decades, there is still a lack of effective treatment options that successfully reduce mortality or improve outcomes in spontaneous ICH patients. Patients who survive the acute phase of pathology often have long-term cognitive dysfunction, which aggravates the burden placed on family and society (Koivunen et al., 2015).

In general, patients experience two pathological processes after ICH onset: primary brain injury and secondary brain injury. Primary brain injury occurs within the first few minutes after bleeding. The expansion of the hematoma, which directly impacts on patient outcomes, plays a pivotal role in this phase (Keep et al., 2012). However, because the efficacy of early surgical removal of hematoma has not been shown convincingly by the International Surgical Trial in Intracerebral Hemorrhage (Mendelow et al., 2005), researchers have begun to focus on secondary brain injury in an attempt to explore pathological processes and discover novel therapeutic strategies. Secondary brain injury following ICH may be triggered by the presence of intraparenchymal blood, and multiple biological changes subsequently occur in this phase, including activation of cytotoxic, excitotoxic, oxidative, and inflammatory pathways (Felberg et al., 2002; Huang et al., 2002; Aronowski and Zhao, 2011). Because the blood-brain barrier is usually disrupted after ICH onset, there is infiltration of neutrophils and various immunocytes, which are recruited from the peripheral circulation. Therefore, systemic and localized inflammation responses play a pivotal role in the pathological processes and recovery of ICH (Latour et al., 2004; Liebner et al., 2018).

Of the treatment options for ICH that have had promising results in pre-clinical trials, neural stem cell (NSC) transplantation has been shown to effectively ameliorate neurological deficits in animals with stroke. NSCs have potent capacities for self-renewal and multiple differentiations (Hara et al., 2008). However, the mechanisms, especially with regards to how NSCs differentiate directionally into functional neural cells, are not well understood; this is a key issue that demands a prompt solution when considering clinical applications. Comprehensive pathological changes occur locally and systemically post-ICH, and inflammation-related microenvironment changes might interact with NSC differentiation, further influencing neurological outcomes (Navarro Quiroz et al., 2018; Peruzzotti-Jametti et al., 2018).

Several cytokines from the interleukin (IL) family, including IL-1 $\beta$ , IL-6, IL-8, and IL-10, have been extensively

investigated for their roles in the pathogenesis of ICH (Ye et al., 2018). IL-17, a cytokine predominantly secreted from T-cell receptor (TCR)  $\gamma\delta$  cells, are significantly associated with the pathological processes of stroke in experimental animal models (Zhong et al., 2016; Arunachalam et al., 2017). Moreover, IL-17 neutralization has been demonstrated to be effective in some central nervous system diseases (Wojkowska et al., 2017). However, both the clinical values of IL-17 and the mechanisms of IL-17 in ICH pathogenesis remain unclear. This study first investigated the clinical values of IL-17 among spontaneous ICH patients, and then explored the potential effects of IL-17 in the pathogenesis of ICH *in vivo* and in neurogenesis *ex vivo*.

## Materials and Methods

### Participants and sample collection

A total of 45 spontaneous ICH patients and 60 age- and sex-matched healthy controls were recruited from the First Affiliated Hospital of Anhui Medical University, China, from January 2017 to March 2018. ICH was diagnosed with two senior neurosurgeons according to the Diagnostic Criteria for Spontaneous Intracerebral Hemorrhage in Adults (WS320-2010).

The inclusion criteria for spontaneous ICH patients were as follows: (1) clear radiological evidence for ICH (round or irregular-shaped high-density focus in computed tomography); (2) bleeding volume was higher than 20 mL; (3) patients were admitted to the emergency room within 4 hours of symptom onset.

The exclusion criteria for spontaneous ICH patients were: (1) subarachnoid hemorrhage or other types of intracranial hemorrhage; (2) severe systemic dysfunctions, malignant tumors, or autoimmune diseases; (3) other central neurological system diseases or mental disturbances.

Healthy subjects were recruited from the physical examination center and were age- and sex-matched.

The exclusion criteria for healthy subjects were: (1) central neurological system diseases or mental disturbances; (2) malignant cancer, autoimmune diseases, or systemic dysfunctions.

Serum from spontaneous ICH patients and healthy controls was collected at the time of admission (day 1), as well as on days 3, 7, and 14 after admission. Serum was stored at  $-80^{\circ}\text{C}$ . The extent of neurological injury was assessed using the Glasgow Coma Scale (GCS) for each patient at admission, and the recovery states were assessed using the Glasgow Outcome Scale (GOS) on day 14 after admission. Evaluations were conducted by two experienced senior doctors who were blinded to patient status. Informed consent was obtained from all individual participants or their family members for inclusion in the study. This study was approved by the Clinical Research Ethics Committee of Anhui Medical University of China (approval No. 20170135) in December 2016. All procedures performed in studies involving human participants were in accordance with the 1964 *Declaration of Helsinki* and its later amendments, or comparable ethical standards.

## Animals

Wild-type male C57BL/6 mice aged 10 weeks and weighing  $25.2 \pm 0.6$  g were obtained from the Experimental Animal Center of Anhui Medical University, China (animal license number: SCXK [Wan] 2017-0001). All mice were housed in temperature- and humidity-controlled conditions with 12-hour/12-hour light/dark cycles, with water and food provided regularly. A total of 31 mice (there were 40 mice at the start of the experiment but only 31 survived) were randomly divided into five groups: the ICH ( $n = 7$ ), ICH + NSC ( $n = 7$ ), ICH + vehicle (saline;  $n = 6$ ), ICH + NSC + IL-17 ( $n = 5$ ), and ICH + NSC + IgG1 ( $n = 6$ ) groups. The mortality rates were 12.5% in the ICH group, 12.5% in the ICH + NSC group, 25% in the ICH + vehicle group, 32.5% in the ICH + NSC + IL-17 neutralization group, and 25% in the ICH + NSC + IgG1 group. The probable reasons for the high mortality observed in this experiment were acute brain injury or infection. Mouse serum was collected continuously for 7 days after ICH. Brain tissue samples were collected at 72 hours after the different treatments for each group. All animal handling and experimental protocols were reviewed and approved by the Institutional Animal Care and Use Committee, Anhui Medical University, China (approval No. 20180248) in December 2017. The experimental procedures followed the United States National Institutes of Health Guide for the Care and Use of Laboratory Animals (NIH Publication No. 85-23, revised 1996).

## ICH mouse models

The experimental mouse model of ICH was based on a previous study (Mao et al., 2017). Briefly, mice were anesthetized with 3.5 % chloral hydrate and placed in a stereotaxic frame. A midline incision was made through the scalp to expose the skull. An injection was made stereotaxically into the caudate nucleus with a syringe at the following coordinates: 0.8 mm anterior, 2.3 mm right lateral, and 3.5 mm deep. Body temperature was maintained at 37°C throughout surgery using a heating pad. The ICH group received an injection of 25  $\mu$ L of autologous blood collected from the tail vein, which was not pretreated with an anticoagulant. The modified neurological severity score was used to evaluate the success of ICH modeling (Su et al., 2017). Mice had free access to food and water after regaining consciousness. Any mice that died during ICH processing were excluded from the study.

## NSC transplantation and anti-IL-17 monoclonal antibody neutralization (mice, *in vivo*)

The methodology for mouse NSC (NE-4C, Cat. No. SCSP-1501, Cell Bank of Chinese Academy of Science, Shanghai, China) transplantation was based on a previous study (Wakai et al., 2014). At 3 hours after experimental ICH was performed, 2  $\mu$ L of NSCs, with a cell concentration of  $2 \times 10^5$ /L, were injected at the injury location using stereotaxic injection instrument (JK023, Jingyuankechuang Co., Beijing, China) in the ICH + NSC group. As a control, mice were injected with 2  $\mu$ L of saline in the ICH + vehicle group.

Purified anti-mouse IL-17A neutralizing antibody (Pro-

tein Accession NP 034682.1; Cat. No. OACD04595) was purchased from Aviva Systems Biology (San Diego, CA, USA). The dose and route for IL-17 neutralization were in accordance with a previous study (Arunachalam et al., 2017). Neutralizing anti-IL-17 antibody was dissolved in phosphate-buffered saline buffer (1:100) and was intraperitoneally injected into the mice at a dose of 16.6 mg/kg body weight during NSC transplantation in the ICH + NSC + IL-17 group. Mouse isotype-control antibody (IgG1; Cat. No. ab81032; Abcam, Cambridge, MA, USA) was used with the same concentration (diluted in phosphate-buffered saline at 1:100).

## Acute brain edema measurement (mice, *in vivo*)

Brain water content was measured at 72 hours after ICH by calculating the ratio of dry to wet brain weight (Tejima et al., 2007). For the wet weight, two hemispheres from different groups of experimental mice were removed, gently blotted on filter paper, and weighed on an electronic balance. Brains were then dried at 100°C in a vacuum oven for 48 hours and reweighed to obtain the dry weight. Water content (%) was calculated using the formula: [(wet weight – dry weight) / wet weight]  $\times$  100.

## Behavior evaluation (mice, *in vivo*)

Two trained investigators, blinded to the animal groups, evaluated neurological deficits before ICH induction and at 72 hours after ICH using a modified neurological severity score (Yang et al., 2016). The scale mainly consisted of five parts: motor tests, sensory tests, beam balance tests, presence or absence of reflexes, and abnormal movements. Functional neurological status was scored on a scale from 1 to 18, with a higher score indicating more severe neurological injuries.

## Flow cytometry analysis and TCR $\gamma\delta$ cell isolation (mice, *ex vivo*)

After sacrificing the experimental mice at 72 hours after ICH, brain peri-hematoma tissue was harvested and suspended in RPMI-1640 medium. The tissue was then digested in a shaker at 37°C, rotating at  $950 \times g$ , for 5 minutes with the addition of type IV collagenase (1 mg/mL) and DNase I (50 mg/mL). Cell supernatants were then removed, resuspended, isolated by centrifugation, and washed with RPMI-1640 prior to flow cytometry. The final cell amount was equivalent in both groups, with a concentration of  $2 \times 10^6$ /mL. Cells from brain peri-hematoma tissue were incubated with fluorescence-labeled antibodies against the surface markers IL-17-APC-Cy7 (Cat. No. 560821; BD Biosciences, San Jose, CA, USA) and TCR  $\gamma\delta$ -FITC (Cat. No. 559501; BD Biosciences). Incubations were carried out according to the manufacturer's protocols, at 4°C for 40 minutes in the dark.

In addition, TCR  $\gamma\delta$  cells were isolated from circulating peripheral blood mononuclear cells of C57BL/6 mice. After cell suspension of peripheral blood mononuclear cells, TCR  $\gamma\delta$ -FITC antibody was added to the suspension and incubated in the dark for 40 minutes. The infiltration of the fluorescence-labeled suspension was then tested. Fluores-

cence-activated cell sorting analysis was performed using a CytoFLEX flow cytometer (Beckman Coulter, Brea, CA, USA), and data were analyzed using FlowJo software 7.6.1 (FlowJo LLC, Ashland, OR, USA).

#### **Enzyme-linked immunosorbent assay (cells, mice, and humans, *in vitro*)**

IL-17 levels in the serum of humans (consecutively for 14 days) and mice (consecutively for 7 days), as well as suspensions of different cell culture/co-cultured groups (at 7 days after cell culture), were measured with enzyme-linked immunosorbent assay kits according to the manufacturer's protocols and based on the quantitative sandwich enzyme immunoassay technique. Briefly, cell cultures were centrifuged for 20 minutes at  $300 \times g$  and supernatant was collected. Fifty microliters of human serum, mouse serum, or supernatant were then separately added to the enzyme-linked immunosorbent assay plates and incubated for 30 minutes at 37°C. The plates were washed and the conjugating reagent was added. After the incubation and washing processes, chromogenic agents were added, followed by stop solution. The concentrations of IL-17 were determined using a standard curve obtained using standardized protein. The absorbance of each well was read at 450 nm using an enzyme-linked immunosorbent assay reader (Bio-Tek, Winooski, VT, USA).

#### **Western blot assay (cells, *in vitro*)**

Cells were lysed at 7 days after cell culture with cold lysis buffer containing protease inhibitors, and total proteins were then extracted using a RIPA buffer kit (Beyotime Biotechnology, Shanghai, China) according to the manufacturer's protocol. The concentration of proteins was detected using a bicinchoninic acid protein kit (Beyotime Biotechnology). The proteins were separated on 10% sodium dodecyl sulfate polyacrylamide gel electrophoresis and moved to polyvinylidene difluoride membranes (Millipore Corp., Bedford, MA, USA). The membranes were blocked with 5% non fat milk (w/v) dissolved in Tris-buffered saline with Tween for 1 hour at room temperature, and then labeled with primary antibodies: rabbit anti-mouse Nestin antibody (a neuroepithelial stem cell biomarker; dilution 1:1000; Cat#. ESAP12392; Elabscience, Wuhan, China), rabbit anti-mouse glial fibrillary acidic protein (GFAP) antibody (an astrocyte biomarker; dilution 1:2000; Cat#. ENT1894; Elabscience), rabbit anti-mouse microtubule-associated protein 2 (MAP2) antibody (a neuron biomarker; dilution 1:1000; Cat#. ESAP12886; Elabscience), and  $\beta$ -actin, at 4°C overnight followed by incubation with secondary goat anti-mouse IgG (H+L) (peroxidase/horseradish peroxidase conjugated) antibody (dilution 1:1000; Cat#. E-AB-1001; Elabscience) for 1.5 hours at room temperature. The protein bands were visualized and captured using a Tanon 1600R imaging system (Tanon Technology Co., Ltd., Shanghai, China). The optical density of each band was quantified using ImageJ software (NIH, Bethesda, MD, USA) and normalized to the intensity of  $\beta$ -actin.

#### **Nissl staining (mice, *in vitro*)**

Nissl staining solution (Cat. No. C0117) was purchased from Beyotime Biotechnology (Shanghai, China). Ten-micron thick fresh frozen brain sections were prepared 72 hours after ICH and stained with the Nissl staining solution for 5 minutes, as per the manufacturer's protocol. After two brief washes with distilled water, sections were dehydrated in 95% ethyl alcohol and cleared with xylene. Pictures were taken using a fluorescence microscope (BX61; Olympus, Tokyo, Japan). Five fields were randomly chosen at 400 $\times$  magnification for each brain section and the absolute numbers of Nissl bodies were counted and calculated.

#### **Terminal deoxynucleotidyl transferase-mediated dUTP nick end labeling (mice, *in vitro*)**

Cell death was detected using a terminal deoxynucleotidyl transferase-mediated dUTP nick end labeling (TUNEL) kit (Cat. No. 11684795910; Roche, Basel, Switzerland). Brain sections were prepared at 72 hours after ICH and incubated with the terminal deoxyribonucleotidyl transferase (TdT) enzyme and reaction mixture at 37°C for 1 hour in a humid atmosphere. The converter-POD was added and sections were incubated in a humid chamber at 37°C for 30 minutes. After coloration using diaminobenzidine (DAB) chromogenic agents, incubated at room temperature for 10 minutes, the nuclei were stained using hematoxylin. TUNEL-positive cells exhibited fluorescence by incorporating fluorescein-12-dUTP at the 3'-OH ends of fractured DNA under the catalytic circumstances brought about by TdT. Pictures were taken using a light microscope (Olympus). Five fields were randomly chosen at 400 $\times$  magnification in each brain section, and the absolute numbers of TUNEL-positive cells were then counted and calculated.

#### **Cell culture/co-culture media (cells, *ex vitro*)**

The mouse NSC line (NE-4C; Cat. No. SCSP-1501) was obtained from the Cell Bank of the Chinese Academy of Science (Shanghai, China). Three groups of cell culture/co-culture media were included. NSC culture medium: Frozen NE-4C cell lines were pretreated in a 37°C water bath to defrost. The NE-4C cells were then incubated in 2 mL of Dulbecco's modified Eagle's medium containing 1% penicillin-streptomycin, 1% glutamax, and 1% non-essential amino acid, with 10% heat-inactivated fetal bovine serum, in a humid incubator at 37°C with 5% CO<sub>2</sub> and 95% air for 20 minutes. NSC + TCR  $\gamma\delta$  cell medium: TCR  $\gamma\delta$  cells were added to the NSC culture medium at a ratio of NE-4C:TCR  $\gamma\delta$  cells of 1:5, and then co-cultured for 24 hours. NSC + TCR  $\gamma\delta$  cells + IL-17 neutralization medium: Neutralizing anti-IL-17 monoclonal antibody (mAb) at a concentration of 2  $\mu$ g/mL was added to the NSC + TCR  $\gamma\delta$  cell medium, and the cells were co-cultured for 24 hours.

#### **Cell viability assay (cells, *ex vitro*)**

Cell proliferation was assessed using a CCK-8 assay according to the manufacturer's protocol for the CCK-8 kit (Cat#. 96992; Sigma, St Louis, MO, USA) at 7 days after cell culture.

Three groups of cells (NE-4C cells, co-cultured NE-4C/TCR  $\gamma\delta$  cells, and co-cultured NE-4C/TCR  $\gamma\delta$ /IL-17 neutralization cells) were incubated in 96-well plates. Next, 90  $\mu$ L of fresh culture media and 10  $\mu$ L of CCK-8 solution were separately added to each sample. Cells were then incubated at 37°C for 2 hours. Optical density values were determined using a microplate reader at 450 nm.

### Statistical analysis

SPSS 19.0 software (IBM Co., Ltd., Armonk, NY, USA) was used for statistical analysis. All enumeration data are given as the mean  $\pm$  standard deviation (SD) and were analyzed by a Student's *t*-test or one-way analysis of variance analysis followed by a Bonferroni *post hoc* test. The correlations of GOS and GCS measurement data with serum IL-17 concentrations on the day of admission were calculated using Pearson correlation analysis.  $P < 0.05$  was considered statistically significant.

## Results

### Serum IL-17 levels are elevated in spontaneous ICH patients and correlate with neurological recovery (humans, *in vitro*)

To investigate the clinical values of IL-17 in the pathological processes of spontaneous ICH, human serum IL-17 levels were dynamically tested at different time points following ICH. Serum IL-17 levels peaked in ICH patients at day 3 and then decreased, but levels remained significantly higher than in healthy controls (Figure 1). We also performed a correlation analysis of serum IL-17 levels and both neurological damage and recovery, using GCS and GOS, respectively. There were no correlations between serum IL-17 level at admission and GCS ( $r = -0.211$ ,  $P = 0.105$ ), but there was a significant negative correlation between serum IL-17 on day 14 and GOS ( $r = -0.498$ ,  $P < 0.01$ ; Figure 2).

### Serum IL-17 levels are elevated in an ICH mouse model (mice, *in vitro*)

Serum IL-17 levels were elevated in the ICH mouse model on day 2 post-ICH. These levels peaked on day 3 and subsequently decreased on day 7, although values were still high compared with controls (Additional Figure 1).

### NSC transplantation reduces IL-17 levels (mice, *ex vivo*)

In an experimental mouse model of ICH, we examined the co-expression of both IL-17<sup>+</sup> and TCR  $\gamma\delta$ <sup>+</sup> cells in peri-hematoma tissue using intracellular cytokine staining of the ICH and ICH + NSC groups at day 3. Overall, IL-17<sup>+</sup> cells were significantly reduced in the ICH + NSC group compared with the ICH group ( $P = 0.01$ ), while there were no significant differences in TCR<sup>+</sup> cells between these two groups ( $P = 0.061$ ). In addition, the proportion of TCR  $\gamma\delta$ /IL-17<sup>+</sup> cells was significantly higher in the ICH group than in the ICH + NSC group ( $P = 0.002$ ). The proportion of cells co-expressing TCR  $\gamma\delta$  and IL-17 was slightly higher in the ICH group than in the ICH + NSC group ( $P = 0.045$ ). There were no significant differences in TCR  $\gamma\delta$ /IL-17<sup>-</sup> and TCR

$\gamma\delta$ <sup>+</sup>/IL-17<sup>-</sup> cells between the two groups ( $P > 0.05$ ; Figure 3).

### IL-17 neutralization ameliorates neurological damage in three experimental ICH groups (mice, *in vitro* and *in vivo*)

There were no significant differences in modified neurological severity score evaluations, brain edema measurements, TUNEL staining, or Nissl staining between the ICH and ICH + vehicle groups, or between the ICH + NSC and ICH + NSC + IgG1 groups.

Neurological damage and recovery were assessed in the ICH + vehicle group, the ICH + NSC group, and the ICH + NSC + IL-17 group using several tests.

In the brain edema assay, NSC transplantation reduced edema volume compared with the ICH-only mice ( $P = 0.037$ ). However, there was no difference in edema content between the ICH + NSC and ICH + NSC + IL-17 groups ( $P = 0.199$ ; Figure 4A).

Behaviors were evaluated among the three groups using the modified neurological severity score. NSC transplantation ameliorated neurological damage ( $P = 0.003$ ). Similarly, simultaneous treatment with both NSC transplantation and IL-17 neutralization enhanced neurological recovery ( $P = 0.042$ ; Figure 4B).

Cell death in the peri-hematoma region was evaluated by TUNEL staining on day 3 after ICH. There was noticeable brain tissue damage and cell death around the hematoma. However, NSC transplantation ameliorated cell death, and the simultaneous use of IL-17 neutralization enhanced this amelioration. Compared with the experimental controls (ICH), TUNEL-positive cells were reduced by 25–30% ( $P < 0.001$ ) in the ICH + NSC group and by 30–40% ( $P = 0.013$ ) in the ICH + NSC + IL-17 group, by absolute number per survey field (Figure 5).

Functional neural cells were also assessed using Nissl staining. Absolute numbers of Nissl bodies were  $22.17 \pm 6.30$  in the ICH group,  $39.33 \pm 5.25$  in the ICH + NSC group, and  $48.83 \pm 7.03$  in the ICH + NSC + IL-17 group in each field. There were significant differences between the ICH and ICH + NSC groups ( $P < 0.001$ ) as well as between the ICH + NSC and ICH + NSC + IL-17 groups ( $P = 0.024$ ). We also observed many small-sized Nissl bodies in the ICH group, relative to the other two groups (Figure 6).

### IL-17 neutralization eliminates the adverse effects of NSC viability caused by IL-17 secreted by TCR $\gamma\delta$ cells (cells, *ex vivo*)

In the cell co-culture mediums, we tested whether using anti-IL-17 mAb could effectively neutralize functional IL-17 concentration, which was predominantly secreted by TCR  $\gamma\delta$  cells in the co-cultured mediums. IL-17 levels were tested using enzyme-linked immunosorbent assay (Additional Figure 2). The IL-17 produced by TCR  $\gamma\delta$  cells could be efficiently blocked by anti-IL-17 mAb.

Cell viabilities were assessed using a CCK-8 test at 72 hours in the three groups. Cell viability decreased under TCR  $\gamma\delta$  cell co-culture ( $P = 0.023$ ). However, IL-17 neutralization ameliorated this effect and increased cell viability

compared with the NSC + TCR  $\gamma\delta$  co-cultured cell group ( $P = 0.031$ ; **Additional Figure 3**).

#### **Function of IL-17 secreted by TCR $\gamma\delta$ cells and IL-17 neutralization in NSC differentiation (cells, *ex vivo*)**

Nestin, MAP2, and GFAP antibodies were used to evaluate the impacts of IL-17 and IL-17 neutralization in NSC differentiation among the three groups. Nestin expression was upregulated in the NSC + TCR  $\gamma\delta$  co-cultured cell group compared with the control (NSC culture) group ( $P < 0.01$ ). Compared with the NSC + TCR  $\gamma\delta$  co-cultured cell group, Nestin expression was decreased in the NSC + TCR  $\gamma\delta$  + IL-17 neutralization co-cultured cell group ( $P = 0.002$ ). Expression of GFAP was decreased in the NSC + TCR  $\gamma\delta$  co-cultured cell group compared with the control group ( $P = 0.003$ ), while IL-17 neutralization increased GFAP expression ( $P = 0.015$ ). MAP2 expression was decreased in the NSC + TCR  $\gamma\delta$  co-cultured cell group. However, there were no significant differences in MAP2 expression between the NSC + TCR  $\gamma\delta$  co-cultured cell group and the NSC + TCR  $\gamma\delta$  + IL-17 neutralization co-cultured cell group ( $P = 0.098$ ; **Figure 7**).

#### **Discussion**

NSCs are a unique population of cells with self-renewal and multi-potent properties, and they can differentiate into several cell lineages, including neurons, astrocytes, and oligodendrocytes (Yang et al., 2019; Zhang et al., 2019). In normal conditions, NSCs reside in the subventricular and subgranular zones of the brain and do not actively differentiate, but these cells play key roles in every stage of brain development (Coronel et al., 2019). The inactive forms of NSCs are reported to become activated after brain damage and may be involved in the process of brain repair. However, the reported self-repair effects are usually transient, and are inadequate against the pathological processes (Huang and Zhang, 2019). Therefore, increasing numbers of investigations into NSCs in brain damage have been conducted in recent decades, aiming to discover potential strategies to both activate endogenous NSCs and transplant exogenous NSCs, in an attempt to promote neurorestorative processes (Chen et al., 2014; Encinas and Fitzsimons, 2017). We previously reported that neuroinflammation has a fundamental role in the processes of secondary brain injury in ICH microenvironments. Multiple anti-inflammatory and pro-inflammatory cytokines have been reported to be involved in the processes of both neurological damage and repair, exerting comprehensive and interactive effects in the differentiation of transplanted NSCs (Zhang et al., 2018).

IL-17, also known as IL-17A, with a solid linkage between innate and adaptive immunity, has been reported to exert both deleterious and beneficial effects in neuroinflammation (Kolls and Linden, 2004). However, few studies have reported clinical values for both diagnosis and prognosis in ICH. A multi-center investigation in Europe reported that circulating IL-17 levels may not be a candidate biomarker to distinguish real stroke from disorders that mimic stroke in the super-acute phase of ICH or cerebral ischemia (Bustamante et

al., 2017). Compared with several biomarkers that have immediate responses in the earliest stage of ICH, such as IL-4 and IL-10 (Liu et al., 2015; Wang et al., 2016), we found that serum IL-17 level was significantly elevated on day 3 post-ICH. In addition, we failed to find any association between serum IL-17 levels and neurological damage as assessed by GCS evaluation at admission in spontaneous ICH patients, indicating that IL-17 might respond relatively slowly in the pathological process. However, a higher serum IL-17 level at day 14 indicated a poorer recovery among spontaneous ICH patients using GOS evaluation. These results suggest that IL-17 may have a neurotoxic role in the pathological processes of ICH, and effectively influence disease outcomes.

As a main producer of IL-17, the roles of TCR  $\gamma\delta$  cells in ischemic stroke have been well documented, and include the mediation of neurotoxic roles and the aggravation of ischemic brain injury by generating various chemotactic signals for peripheral myeloid cells, such as neutrophils and monocytes, and secreting cytokines, including IL-17 (Benakis et al., 2016). In another aspect, results reported by both Gao et al. (2014) and Zhang et al. (2015) suggest that NSC transplantation may decrease TCR  $\gamma\delta$  cell numbers and infiltration after ICH. Because of the inherent relationship between TCR  $\gamma\delta$  cells and IL-17, previous studies have often not identified any distinctions between the two biomarkers in ICH pathogenesis. Our flow cytometry results regarding the co-expression of TCR  $\gamma\delta$  cells and IL-17 in peri-hematoma tissue indicated that it may be IL-17, rather than the TCR  $\gamma\delta$  cells, that has a predominant effect on pathogenesis and neurogenesis in ICH.

Based on this finding, we speculated that the inhibition of excessive pro-inflammatory effects, induced by IL-17 overload, might alleviate the neurotoxic effects of ICH. A previous study reported that the simultaneous application of IL-17 neutralization and therapeutic hypothermia had a better efficacy for ischemic stroke than anti-IL-17 antibody treatment or therapeutic hypothermia alone (Arunachalam et al., 2017). In the present study, NSC transplantation was an effective method that promoted neurological recovery in an experimental mouse model of ICH. Furthermore, the simultaneous application of IL-17 neutralization and NSC transplantation enhanced this protective effect, indicating that IL-17 neutralization effectively promoted the neuroprotective effect induced by NSC transplantation. However, the mechanisms of IL-17 in neurological recovery and directional differentiation of NSCs are controversial, and have only been addressed in very few studies.

Thus, in the present study we explored the potential mechanisms of IL-17 in NSC neurogenesis *ex vivo*. Three proteins, Nestin, MAP2, and GFAP, were used here to distinguish NSC differentiation in the different co-cultured cell media. Nestin was used as a biomarker for neuroepithelial stem cells, while GFAP was used as a marker for astrocytes and MAP2 was used as a biomarker for neurons. There was an upregulation of Nestin and a downregulation of GFAP and MAP2 after co-culturing TCR  $\gamma\delta$  cells with NSCs. The neutralization of IL-17 with anti-IL-17 mAb antagonized the functions of

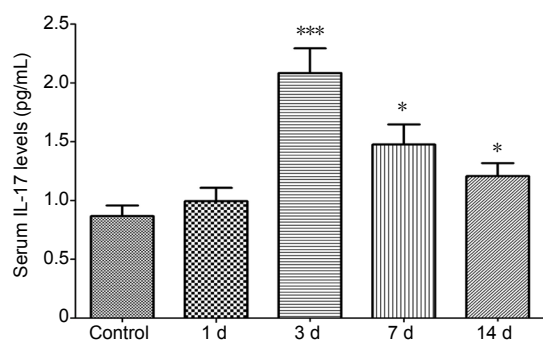


**Figure 1** Dynamic changes of serum IL-17 levels detected by enzyme-linked immunosorbent assay at admission (day 1), day 3, day 7, and day 14 after admission in spontaneous intracerebral hemorrhage patients as well as healthy subjects.

\* $P < 0.05$ , \*\*\* $P < 0.001$ , vs. control group. Data are presented as the mean  $\pm$  standard deviation (SD) ( $n_{\text{case}} = 45$ ,  $n_{\text{control}} = 60$ ; one-way analysis of variance analysis followed by Bonferroni *post hoc* test). IL-17: Interleukin 17.

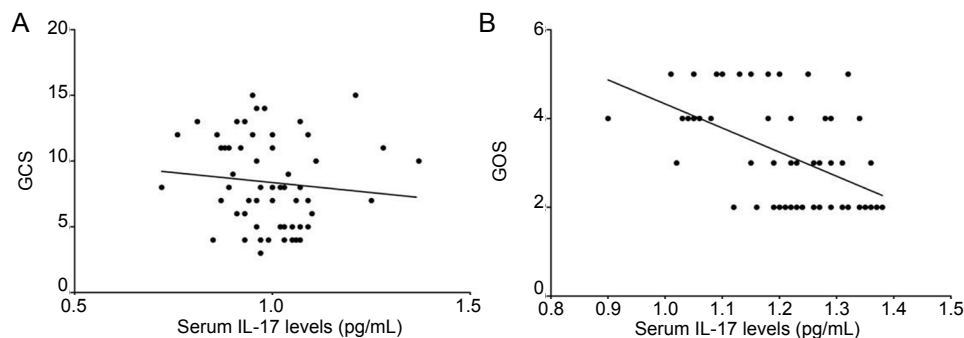


**Figure 2** Correlation of serum IL-17 levels with GCS and GOS in spontaneous intracerebral hemorrhage patients.

(A) GCS at admission; (B) GOS at day 14 ( $n = 45$ ; Pearson correlation analysis). GCS: Glasgow Coma Scale; GOS: Glasgow Outcome Scale; IL-17: interleukin 17.

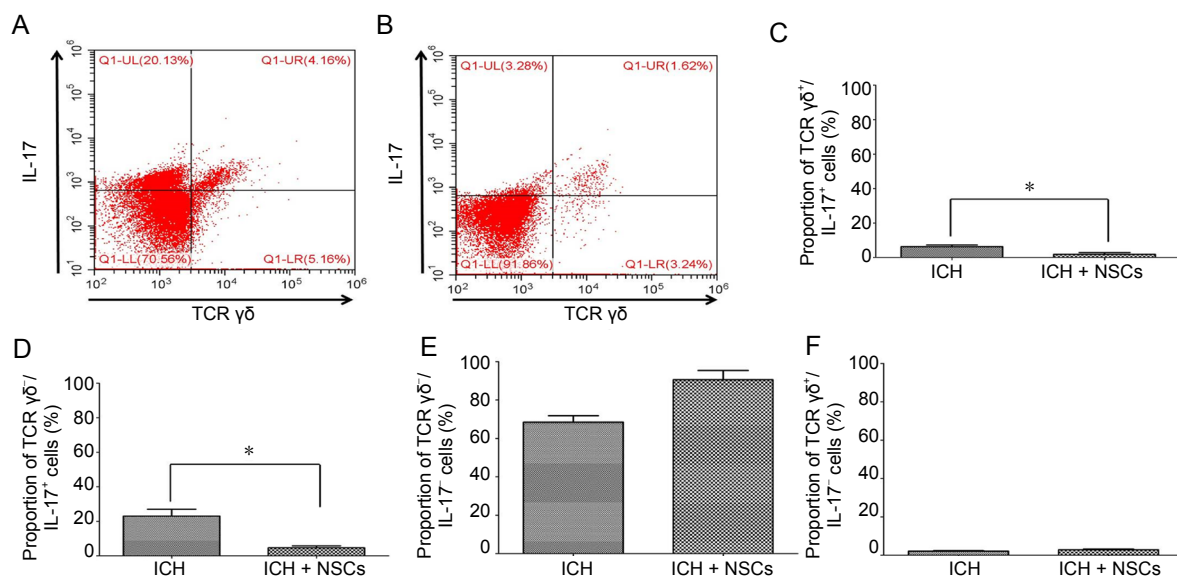


**Figure 3** Flow cytometry of TCR  $\gamma\delta$ /IL-17 co-expression at 72 hours in ICH mice.

(A, B) Flow cytometry of the ICH (A) and ICH + NSC (B) groups. (C) The proportion of TCR  $\gamma\delta^+$ /IL-17 $^+$  co-expression was slightly higher in the ICH group than in the ICH + NSC group. (D) The proportion of TCR  $\gamma\delta^+$ /IL-17 $^-$  cells was significantly higher in the ICH group than in ICH + NSC group. (E, F) There were no significant differences in TCR  $\gamma\delta^-$ /IL-17 $^+$  (E) and TCR  $\gamma\delta^-$ /IL-17 $^-$  cells (F) between the two groups. \* $P < 0.05$ . Data are presented as the mean  $\pm$  SD ( $n = 6$ , Student's *t*-test). ICH: Intracerebral hemorrhage; IL-17: interleukin 17; NSCs: neural stem cells.

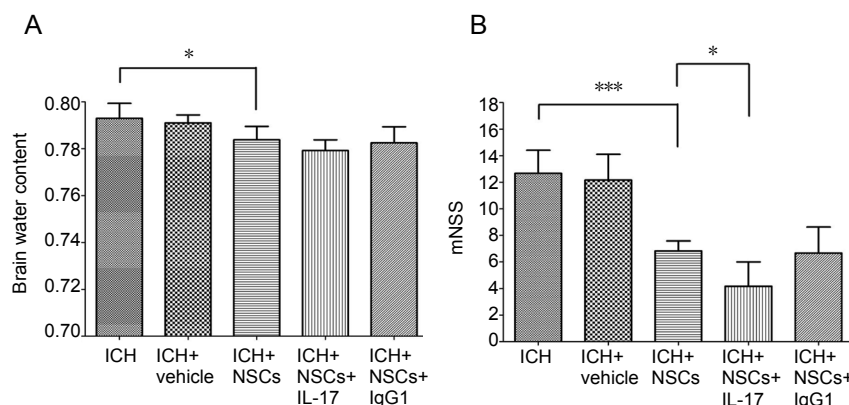


**Figure 4** Brain water content and mNSS among different groups of experimental ICH mice at 72 hours post ICH.

(A) Brain water content; (B) mNSS. \* $P < 0.05$ , \*\*\* $P < 0.001$ . Data are presented as the mean  $\pm$  SD ( $n = 6$ ; one-way analysis of variance analysis followed by Bonferroni *post hoc* test). ICH: Intracerebral hemorrhage; IL-17: interleukin 17; mNSS: modified neurological severity score; NSCs: neural stem cells.

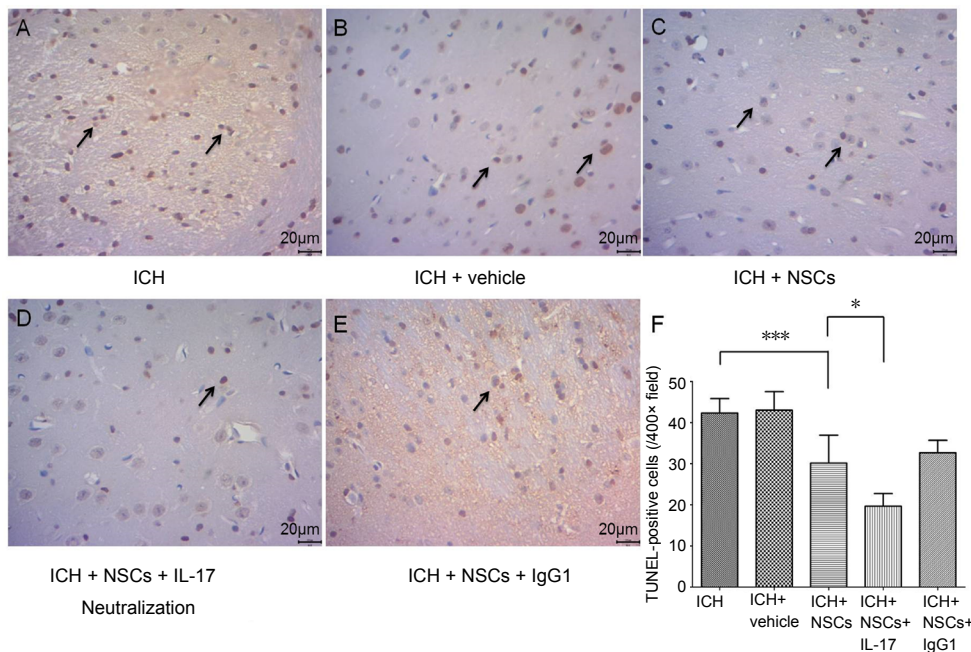


**Figure 5** TUNEL-positive cells revealed cell death of brain cells in different groups of experimental ICH mice at 72 hours post-ICH. (A) ICH group, (B) ICH + vehicle group, (C) ICH + NSC group, (D) ICH + NSC + IL-17 group, and (E) ICH + NSC + IgG1 group. Arrows: TUNEL-positive cells. Original magnification, 400 $\times$ . Scale bars: 20  $\mu$ m. (F) TUNEL-positive cell counts in assay areas. \* $P < 0.05$ , \*\*\* $P < 0.001$ . Data are presented as the mean  $\pm$  SD ( $n = 6$ ; one-way analysis of variance analysis followed by Bonferroni *post hoc* test). ICH: Intracerebral hemorrhage; IL-17: interleukin 17; NSCs: neural stem cells.

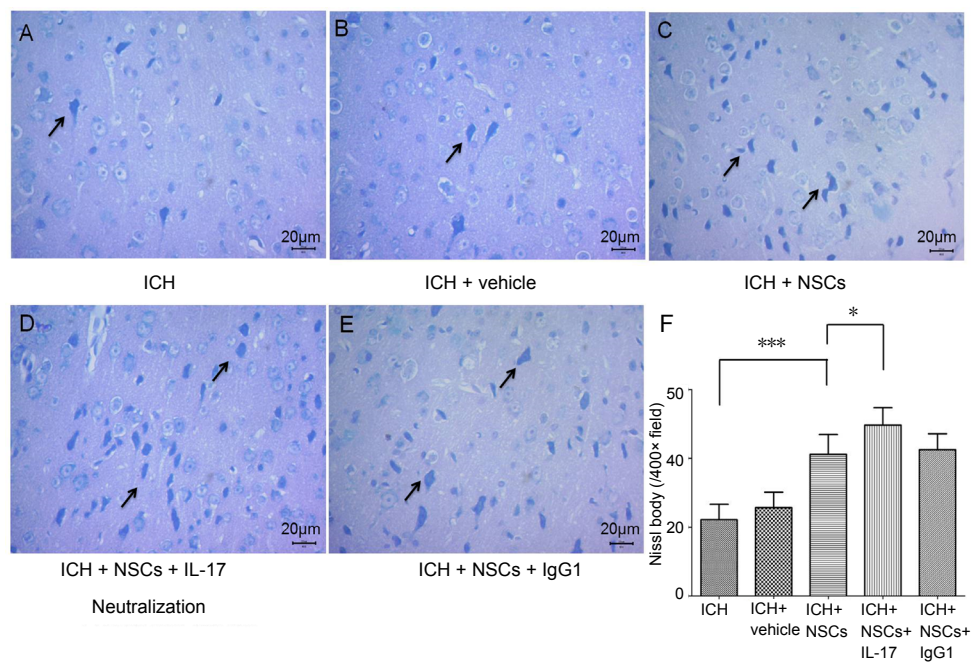


**Figure 6** Nissl staining reveals tissue damage in the hematoma area in different groups of experimental ICH mice at 72 hours post-ICH. (A) ICH group, (B) ICH + vehicle group, (C) ICH + NSC group, (D) ICH + NSC + IL-17 group, and (E) ICH + NSC + IgG1 group. Arrows: Nissl body. Original magnification, 400 $\times$ . Scale bars: 20  $\mu$ m. (F) Nissl body counts in assay areas (F). \* $P < 0.05$ , \*\*\* $P < 0.001$ . Data are presented as the mean  $\pm$  SD ( $n = 6$ ; one-way analysis of variance analysis followed by Bonferroni *post hoc* test). ICH: Intracerebral hemorrhage; IL-17: interleukin 17; NSCs: neural stem cells.

TCR  $\gamma\delta$  cells on NSC differentiation. However, this effect was not observed with MAP2 protein. These results indicate that the IL-17 secreted by TCR  $\gamma\delta$  cells may have important effects on NSC differentiation, inhibiting the differentiation of NSCs into astrocytes and neurons. The neutralization of IL-17 by anti-IL-17 mAb might relieve the inhibitory effect on the differentiation of astrocytes, rather than neurons. Although stroke can trigger NSCs to differentiate from an inactive form, the migration and proliferation of NSCs can be inhibited, which may lead to failures in spontaneous demyelination and neural repairs by NSCs in the inflamed foci. It has been reported in several investigations that IL-17 may have paradoxical roles with NSCs. Lin et al. (2016) found that in the post-stroke stage, astrocytic IL-17A maintained and enhanced the survival and differentiation of subven-

tricular zone neural precursor cells, as well as subsequent synaptogenesis and functional recovery. However, Liu et al. (2014) found that endogenous IL-17 ablated neurogenesis in the adult dentate gyrus of the hippocampus, while this inhibitory effect could be eliminated by genetic deletion of IL-17, which increased the expression of proneuronal genes in neural precursor cells. Additionally, in a study of multiple sclerosis (Li et al., 2013), exogenous IL-17 reduced the numbers of NSCs and their ability to form neurospheres. We hypothesize that the divergence of the effects of IL-17 on NSC neurogenesis may be because of the different origins of IL-17. IL-17 originating from astrocytes might be protective for NSCs, while IL-17 originating from TCR  $\gamma\delta$ /Th17 cells might exert toxic effects on NSCs.

The commercial anti-IL-17 mAb agents, secukinumab and

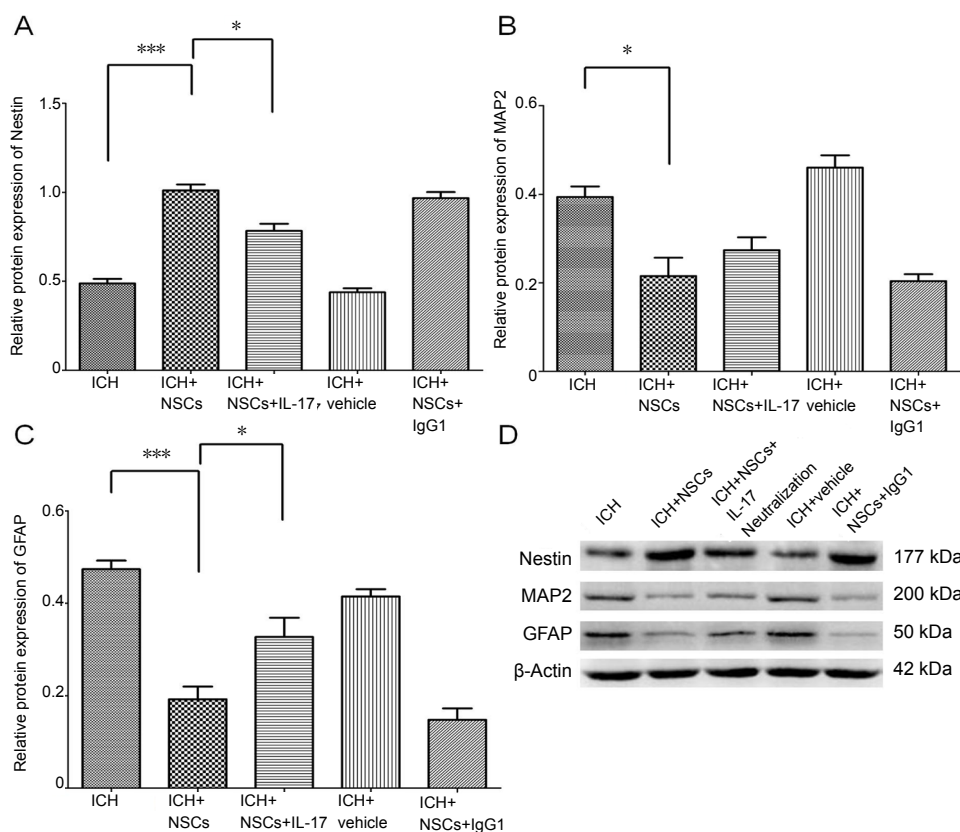


**Figure 7** Expression of Nestin, GFAP and MAP2 in different groups after cell culture/co-culture for 7 days, using western blot assay. (A–D) Western blot images (D) show the expression of Nestin (A), GFAP (B), and MAP2 (C) among different cell culture/co-culture groups. \* $P < 0.05$ , \*\*\* $P < 0.001$ . Data are presented as the mean  $\pm$  SD ( $n = 6$ ; one-way analysis of variance analysis followed by Bonferroni *post hoc* test). GFAP: Glial fibrillary acidic protein; ICH: intracerebral hemorrhage; IL-17: interleukin 17; MAP2: microtubule-associated protein 2; NSCs: neural stem cells.

ixekizumab, have been applied therapeutically in psoriasis, an inflammatory dermatosis. Furthermore, IL-17 neutralization has been investigated in a mechanism study of multiple sclerosis. However, there is no evidence for these commercial agents in the treatment of stroke. We here provided a proof-of-concept, in which anti-IL-17 mAb may be a promising therapeutic agent for the treatment of ICH. Therefore, an investigation into the pharmacological functions of IL-17 in stroke patients is needed.

However, a limitation of this study should be stated. Many studies might consider that the inflammatory cytokines were derived from immunocytes, because an abundance of immunocytes were recruited from circulation and were predominantly located around the injured tissue. However, Li et al. (2017) found that astrocyte-derived IL-17A aggravated ischemic injuries in neurons, probably through its receptor IL-17R, at the early phase of ischemic stroke. Meanwhile, astrocytes may be the target of both Th17 cells and IL-17A in the promotion of inflammatory processes, indicating that astrocytes might be very important in stroke. It may be that, because of their colonization properties, the response of astrocytes to brain injury might be earlier than that of immunocytes. Therefore, more attention should be paid to the immediate inflammatory responses of astrocytes in stroke.

In summary, serum IL-17 levels significantly correlated with recovery in spontaneous ICH patients. In an experimental mouse model of ICH, NSC transplantation reduced IL-17 levels in peri-hematoma tissue and ameliorated neurological deficits. The simultaneous application of neutralizing anti-IL-17 antibodies might further promote the therapeutic

effects of NSC transplantation by relieving the inhibition of NSC differentiation into astrocytes, which was induced by IL-17 secreted by TCR  $\gamma\delta$  cells.

**Author contributions:** Study design: HWC, LG and LY; experimental implementation: PPL, LY, BSW and MS; data analysis: XM, TYS and HQ; paper drafting: LG and PPL; paper reviewing: LY and HWC; fundraising: HWC. All authors approved the final version of the paper.

**Conflicts of interest:** The authors declare that there are no conflicts of interest associated with this manuscript.

**Financial support:** This study was supported by the Natural Science Foundation of Anhui Province of China, No. 1708085MH211 (to HWC); the College Top-notch Talent Foundation of Anhui Province of China, No. KJ2018A0207 (to HWC). The funding sources had no role in study conception and design, data analysis or interpretation, paper writing or deciding to submit this paper for publication.

**Institutional review board statement:** This study was approved by the Clinical Research Ethics Committee of Anhui Medical University of China (For human study: Approval No. 20170135) in December 2016. All procedures performed in studies involving human participants were in accordance with the ethical standards of the institutional and/or national research committee and with the 1964 Declaration of Helsinki and its later amendments or comparable ethical standards. All animal handling and experimentation were reviewed and approved by the Institutional Animal Care and Use Committee of Anhui Medical University (For animal study: Approval No. 20180248) in December 2017. The experimental procedure followed the United States National Institutes of Health Guide for the Care and Use of Laboratory Animals (NIH Publication No. 85-23, revised 1996).

**Copyright license agreement:** The Copyright License Agreement has been signed by all authors before publication.

**Data sharing statement:** Datasets analyzed during the current study are available from the corresponding author on reasonable request.

**Plagiarism check:** Checked twice by iThenticate.

**Peer review:** Externally peer reviewed.

**Open access statement:** This is an open access journal, and articles

are distributed under the terms of the Creative Commons Attribution-Non-Commercial-ShareAlike 4.0 License, which allows others to remix, tweak, and build upon the work non-commercially, as long as appropriate credit is given and the new creations are licensed under the identical terms.

**Open peer reviewer:** Hailong Song, University of Missouri Columbia, USA.

**Additional files:**

**Additional file 1:** Open peer review report 1.

**Additional Figure 1:** Dynamic changes of serum Interleukin 17 (IL-17) level in ICH modeling mice.

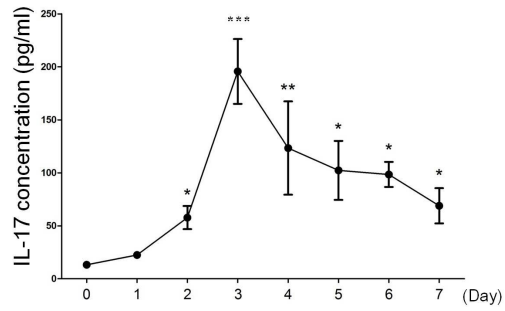
**Additional Figure 2:** Interleukin 17 (IL-17) concentration tests among different cell culture/co-culture groups.

**Additional Figure 3:** Cell viability tests among different cell culture/co-culture groups.

## References

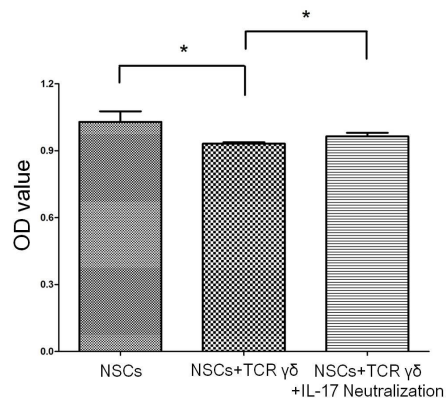
- Aronowski J, Zhao X (2011) Molecular pathophysiology of cerebral hemorrhage: secondary brain injury. *Stroke* 42:1781-1786.
- Arunachalam P, Ludewig P, Melich P, Arumugam TV, Gerloff C, Prinz I, Magnus T, Gelderblom M (2017) CCR6 (CC Chemokine Receptor 6) is essential for the migration of detrimental natural interleukin-17-producing gammadelta T cells in stroke. *Stroke* 48:1957-1965.
- Benakis C, Brea D, Caballero S, Faraco G, Moore J, Murphy M, Sita G, Racchumi G, Ling L, Pamer EG, Iadecola C, Anrather J (2016) Commensal microbiota affects ischemic stroke outcome by regulating intestinal gammadelta T cells. *Nat Med* 22:516-523.
- Bustamante A, López-Cancio E, Pich S, Penalba A, Giral D, García-Bercooso T, Ferrer-Costa C, Gasull T, Hernández-Pérez M, Millan M, Rubiera M, Cardona P, Cano L, Quesada H, Terceño M, Silva Y, Castellanos M, Garces M, Reverté S, Ustrell X, et al. (2017) Blood biomarkers for the early diagnosis of stroke: the stroke-chip study. *Stroke* 48:2419-2425.
- Chen CC, Chen X, Li TC, Lin HL, Chu YT, Lee HC, Cheng YK, Chen DC, Tsai SC, Cho DY, Hsieh CL (2017) PG2 for patients with acute spontaneous intracerebral hemorrhage: a double-blind, randomized, placebo-controlled study. *Sci Rep* 7:45628.
- Chen L, Qiu R, Li L, He D, Lv H, Wu X, Gu N (2014) The role of exogenous neural stem cells transplantation in cerebral ischemic stroke. *J Biomed Nanotechnol* 10:3219-3230.
- Coronel R, Palmer C, Bernabeu-Zornoza A, Monteagudo M, Rosca A, Zambrano A, Liste I (2019) Physiological effects of amyloid precursor protein and its derivatives on neural stem cell biology and signaling pathways involved. *Neural Regen Res* 14:1661-1671.
- Encinas JM, Fitzsimons CP (2017) Gene regulation in adult neural stem cells. Current challenges and possible applications. *Adv Drug Deliv Rev* 120:118-132.
- Felberg RA, Grotta JC, Shirzadi AL, Strong R, Narayana P, Hill-Felberg SJ, Aronowski J (2002) Cell death in experimental intracerebral hemorrhage: the "black hole" model of hemorrhagic damage. *Ann Neurol* 51:517-524.
- Gao L, Lu Q, Huang LJ, Ruan LH, Yang JJ, Huang WL, ZhuGe WS, Zhang YL, Fu B, Jin KL, ZhuGe QC (2014) Transplanted neural stem cells modulate regulatory T, gammadelta T cells and corresponding cytokines after intracerebral hemorrhage in rats. *Int J Mol Sci* 15:4431-4441.
- Hara K, Yasuhara T, Maki M, Matsukawa N, Masuda T, Yu SJ, Ali M, Yu G, Xu L, Kim SU, Hess DC, Borlongan CV (2008) Neural progenitor NT2N cell lines from teratocarcinoma for transplantation therapy in stroke. *Prog Neurobiol* 85:318-334.
- Huang FP, Xi G, Keep RF, Hua Y, Nemoianu A, Hoff JT (2002) Brain edema after experimental intracerebral hemorrhage: role of hemoglobin degradation products. *J Neurosurg* 96:287-293.
- Huang L, Zhang L (2019) Neural stem cell therapies and hypoxic-ischemic brain injury. *Prog Neurobiol* 173:1-17.
- Keep RF, Hua Y, Xi G (2012) Intracerebral haemorrhage: mechanisms of injury and therapeutic targets. *Lancet Neurol* 11:720-731.
- Koivunen RJ, Harno H, Tatlisumak T, Putaala J (2015) Depression, anxiety, and cognitive functioning after intracerebral hemorrhage. *Acta Neurol Scand* 132:179-184.
- Kolls JK, Linden A (2004) Interleukin-17 family members and inflammation. *Immunity* 21:467-476.
- Krishnamurthi RV, Moran AE, Forouzanfar MH, Bennett DA, Mensah GA, Lawes CM, Barker-Collo S, Connor M, Roth GA, Sacco R, Ezzati M, Naghavi M, Murray CJ, Feigin VL, Global Burden of Diseases I, Risk Factors Study Stroke Expert G (2014) The global burden of hemorrhagic stroke: a summary of findings from the GBD 2010 study. *Glob Heart* 9:101-106.
- Latour LL, Kang DW, Ezzeddine MA, Chalela JA, Warach S (2004) Early blood-brain barrier disruption in human focal brain ischemia. *Ann Neurol* 56:468-477.
- Li S, Dai Q, Yu J, Liu T, Liu S, Ma L, Zhang Y, Han S, Li J (2017) Identification of IL-17A-derived neural cell type and dynamic changes of IL-17A in serum/CSF of mice with ischemic stroke. *Neurol Res* 39:552-558.
- Li Z, Li K, Zhu L, Kan Q, Yan Y, Kumar P, Xu H, Rostami A, Zhang GX (2013) Inhibitory effect of IL-17 on neural stem cell proliferation and neural cell differentiation. *BMC Immunol* 14:20.
- Liebner S, Dijkhuizen RM, Reiss Y, Plate KH, Agalliu D, Constantin G (2018) Functional morphology of the blood-brain barrier in health and disease. *Acta Neuropathol* 135:311-336.
- Lin Y, Zhang JC, Yao CY, Wu Y, Abdelgawad AF, Yao SL, Yuan SY (2016) Critical role of astrocytic interleukin-17 A in post-stroke survival and neuronal differentiation of neural precursor cells in adult mice. *Cell Death Dis* 7:e2273.
- Liu B, Hu B, Shao S, Wu W, Fan L, Bai G, Shang P, Wang X (2015) CD163/Hemoglobin oxygenase-1 pathway regulates inflammation in hematoma surrounding tissues after intracerebral hemorrhage. *J Stroke Cerebrovasc Dis* 24:2800-2809.
- Liu Q, Xin W, He P, Turner D, Yin J, Gan Y, Shi FD, Wu J (2014) Interleukin-17 inhibits adult hippocampal neurogenesis. *Sci Rep* 4:7554.
- Mao LL, Yuan H, Wang WW, Wang YJ, Yang MF, Sun BL, Zhang ZY, Yang XY (2017) Adoptive regulatory T-cell therapy attenuates perihematomal inflammation in a mouse model of experimental intracerebral hemorrhage. *Cell Mol Neurobiol* 37:919-929.
- Mendelow AD, Gregson BA, Fernandes HM, Murray GD, Teasdale GM, Hope DT, Karimi A, Shaw MD, Barer DH, investigators S (2005) Early surgery versus initial conservative treatment in patients with spontaneous supratentorial intracerebral haematomas in the International Surgical Trial in Intracerebral Haemorrhage (STICH): a randomised trial. *Lancet* 365:387-397.
- Navarro Quiroz E, Navarro Quiroz R, Ahmad M, Gomez Escorcia L, Villarreal JL, Fernandez Ponce C, Aroca Martinez G (2018) Cell signaling in neuronal stem cells. *Cells* doi: 10.3390/cells7070075.
- Neves JD, Mestriner RG, Netto CA (2018) Astrocytes in the cerebral cortex play a role in the spontaneous motor recovery following experimental striatal hemorrhage. *Neural Regen Res* 13:67-68.
- Peruzzotti-Jametti L, Bernstock JD, Vicario N, Costa ASH, Kwok CK, Leonardi T, Booty LM, Bicci I, Balzarotti B, Volpe G, Mallucci G, Manferrari G, Donega M, Iraci N, Braga A, Hallenbeck JM, Murphy MP, Edenhofer F, Frezza C, Pluchino S (2018) Macrophage-derived extracellular succinate licenses neural stem cells to suppress chronic neuroinflammation. *Cell Stem Cell* 22:355-368.
- Su WS, Wu CH, Chen SF, Yang FY (2017) Low-intensity pulsed ultrasound improves behavioral and histological outcomes after experimental traumatic brain injury. *Sci Rep* 7:15524.
- Tejima E, Zhao BQ, Tsuji K, Rosell A, van Leyen K, Gonzalez RG, Montaner J, Wang X, Lo EH (2007) Astrocytic induction of matrix metalloproteinase-9 and edema in brain hemorrhage. *J Cereb Blood Flow Metab* 27:460-468.
- Wakai T, Sakata H, Narasimhan P, Yoshioka H, Kinouchi H, Chan PH (2014) Transplantation of neural stem cells that overexpress SOD1 enhances amelioration of intracerebral hemorrhage in mice. *J Cereb Blood Flow Metab* 34:441-449.
- Wang XM, Zhang YG, Li AL, Long ZH, Wang D, Li XX, Xia JH, Luo SY, Shan YH (2016) Expressions of serum inflammatory cytokines and their relationship with cerebral edema in patients with acute basal ganglia hemorrhage. *Eur Rev Med Pharmacol Sci* 20:2868-2871.
- Wojkowska DW, Szpakowski P, Glabinski A (2017) Interleukin 17A promotes lymphocytes adhesion and induces CCL2 and CXCL1 release from brain endothelial cells. *Int J Mol Sci* doi: 10.3390/ijms18051000.
- Yang JT, Fang JT, Li L, Chen G, Qin BG, Gu LQ (2019) Contralateral C7 transfer combined with acellular nerve allografts seeded with differentiated adipose stem cells for repairing upper brachial plexus injury in rats. *Neural Regen Res* 14:1932-1940.
- Yang Z, Wang J, Yu Y, Li Z (2016) Gene silencing of MCP-1 prevents microglial activation and inflammatory injury after intracerebral hemorrhage. *Int Immunopharmacol* 33:18-23.
- Ye L, Gao L, Cheng H (2018) Inflammatory profiles of the interleukin family and network in cerebral hemorrhage. *Cell Mol Neurobiol* 38:1321-1333.
- Zhang G, Chen L, Chen W, Li B, Yu Y, Lin F, Guo X, Wang H, Wu G, Gu B, Miao W, Kong J, Jin X, Yi G, You Y, Su X, Gu N (2018) Neural stem cells alleviate inflammation via neutralization of ifn-gamma negative effect in ischemic stroke model. *J Biomed Nanotechnol* 14:1178-1188.
- Zhang H, Shao B, Zhuge Q, Wang P, Zheng C, Huang W, Yang C, Wang B, Su DM, Jin K (2015) Cross-talk between human neural stem/progenitor cells and peripheral blood mononuclear cells in an allogeneic co-culture model. *PLoS One* 10:e0117432.
- Zhang ZY, Yang J, Fan ZH, Wang DL, Wang YY, Zhang T, Yu LM, Yu CY (2019) Fresh human amniotic membrane effectively promotes the repair of injured common peroneal nerve. *Neural Regen Res* 14:2199-2208.
- Zhong Q, Zhou K, Liang QL, Lin S, Wang YC, Xiong XY, Meng ZY, Zhao T, Zhu WY, Yang YR, Liao MF, Gong QW, Liu L, Xiong A, Hao J, Wang J, Zhu (2016) Interleukin-23 secreted by activated macrophages drives  $\gamma\delta$ T cell production of interleukin-17 to aggravate secondary injury after intracerebral hemorrhage. *J Am Heart Assoc* 5:e004340.

P-Reviewer: Song H; C-Editor: Zhao M; S-Editors: Wang J, Li CH; L-Editors: Gardner B, de Souza M, Qiu Y, Song LP; T-Editor: Jia Y



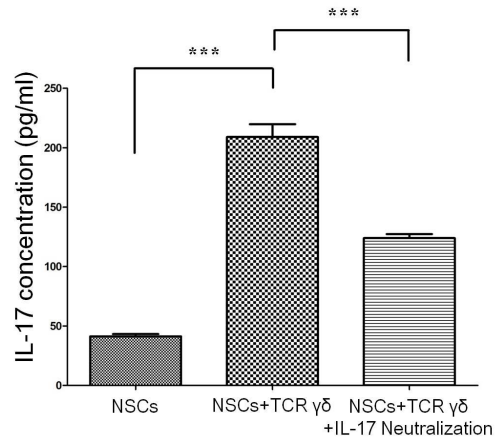
**Additional Figure 1 Dynamic changes of serum Interleukin 17 (IL-17) level in ICH modeling mice.**

\* $P < 0.05$ , \*\* $P < 0.01$ , \*\*\* $P < 0.001$ , vs. 0 day. Data are presented as the mean  $\pm$  SD ( $n=6$ , one-way analysis of variance analysis followed by Bonferroni *post hoc* test). ICH: Intracerebral hemorrhage.



**Additional Figure 2 Interleukin 17 (IL-17) concentration tests among different cell culture/co-culture groups.**

\* $P < 0.05$ . Data are presented as the mean  $\pm$  SD ( $n=6$ , one-way analysis of variance analysis followed by Bonferroni *post hoc* test). NSCs: Neural stem cells; TCR: T cell receptor.



**Additional Figure 3 Cell viability tests among different cell culture/co-culture groups.**

\*\*\*  $P < 0.001$ . Data are presented as the mean  $\pm$  SD ( $n=6$ , one-way analysis of variance analysis followed by Bonferroni *post hoc* test). NSCs: Neural stem cells; TCR: T cell receptor.